

SRI CAT also organized several user science workshops on biological/biomedical applications of x-ray microscopy, polarized x-rays, inelastic x-ray scattering, and nanoscale materials research. New initiatives drawing upon these workshops have resulted in new CATs, such as IXS CAT and Nano-CAT.

Significant accomplishments also took place in the area of user technical support. Staff members from both XFD and ASD completed the final design of the straight section and front end that accommodates the canted undulator setup—the system of choice for new structural biology CATs.

Advanced crystal, zone plate, and mirror x-ray optics have been developed with strong collaboration with the APS user community. Especially noteworthy is the development of profile coating by sputter deposition for the production of aspherical x-ray optical surfaces. This technology has recently been applied to fabricate elliptically shaped Kirkpatrick-Baez mirrors. Also noteworthy is the development and fabrication of a refractory x-ray lens having an adjustable focus.

Significant progress has been made in the area of high-energy x-ray technique development. In particular, the development of high-energy small-angle scattering combined with high-energy wide-angle scattering is proving to be a powerful new technique to study materials systems. The combination of these two techniques allows the gathering of information on texture, strain, and phase with simultaneous information on longer length scales probed by small-angle scattering.

Noteworthy advances were made in both x-ray microscopy techniques and applications,

especially in the biological and materials sciences. Highlights in this report include trace element analysis in marine protists by scanning fluorescence microscopy and microdiffraction imaging of antiferromagnetic domains in chromium.

The program that utilizes polarization properties of x-rays advanced significantly in the last year. As an example, the strength and extent of interlayer exchange coupling and magnetic roughness was measured on Gd/Fe multilayers. This quantitative information was obtained by performing both x-ray resonance exchange scattering (XRES) and x-ray magnetic circular dichroism (XMCD) measurements.

Both SRI-CAT and user technical support have reached a mature state and are prepared for new challenges in the future.

1.2 X-ray Imaging and Optics Development

The effort in x-ray optics and imaging is on development of x-ray interferometers, development of propagation phase-contrast imaging, and high-heat-load optics. In particular, the phase-contrast imaging experiments are being conducted with scientists who were previously not synchrotron users. Through these collaborations, we hope to open a new experimental field to researchers in areas such as entomology.

1.2.1 Fresnel Propagation X-ray Phase-Contrast Imaging

The contrast in this technique is due to Fresnel diffraction. It corresponds to the defocusing technique in electron microscopy and is sensitive to the second derivative of

the phase. Its principal advantage is the simplicity of the setup. Furthermore, submicron resolution is achievable. This technique is made possible by the lateral coherence of the x-ray beam produced by third-generation synchrotron sources.

A drawback of the propagation technique is the nontrivial relationship between the object and the recorded image (actually a Fresnel diffraction pattern). But when a quantitative (numerical) retrieval of the phase is not needed, it can also be used in a qualitative way, namely, in the edge-detection regime.

This technique has been applied to a wide variety of systems. We imaged stainless-steel fuel injectors several millimeters in thickness using 70 keV x-rays (Lee et al., 2001). The results suggest the possibility of time-resolved studies. The superior spatial resolution of this technique allowed the examination of small (micron) crack openings in aluminum samples as a function of applied load. This is being used to help understand roughness-induced fatigue crack closures (Stock et al., submitted).

Phase-contrast imaging is a valuable tool to distinguish between two phases of the same material in a sample. As an example of this, we could see calcite crystal reinforcement at the incisal end of sea urchin teeth, as part of its strengthening and self-sharpening strategies (Stock et al., in press).

Working at relatively high energy (22 keV) with biological samples to reduce absorption, we could keep small insects alive for more than ten minutes and study their feeding and respiration mechanisms (Westneat et al., 2002). For instance, a new mechanism of tracheal pumping in the head and prothorax has been observed. An

example of the images from this work is shown in Fig. 1.1.

1.2.2 X-ray Imaging of Shock Waves Generated by High-Pressure Fuel Sprays

High-pressure, high-speed sprays are an essential technology in many applications, including fuel injection systems, thermal and plasma spray coatings, and liquid-jet machining. These liquid jets, often traveling at supersonic speeds, are optically opaque due to the highly dense liquid droplets surrounding the sprays. The detailed structure of the sprays, which is directly related to their effectiveness, cannot be resolved by optical methods. In the case of fuel injection, an understanding of the structure and dynamics of the jets is critical in optimizing the injection process to increase fuel efficiency and reduce emissions. In collaboration with Cornell University and ANL Energy Systems Division, we have used synchrotron x-radiography and a novel fast x-ray detector

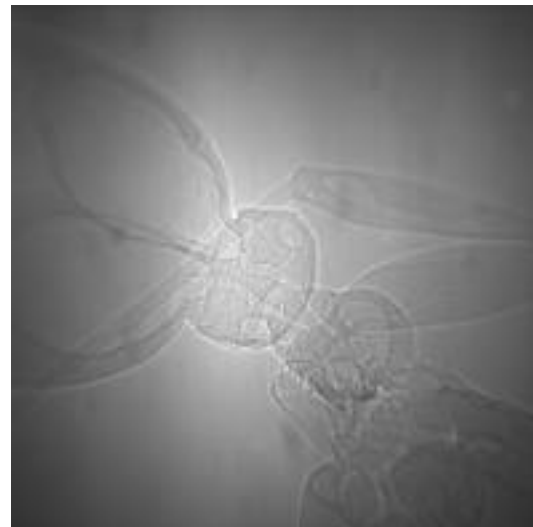


Fig. 1.1. Phase-contrast image of an ant abdomen.

to visualize the transient structure of supersonic diesel fuel sprays generated by high-pressure injection (MacPhee et al., 2002). The generated images allow quantitative analysis of the thermodynamic properties of the shock waves, which had proved to be impossible with optical imaging.

The experimental setup uses a high-pressure common-rail diesel injection system, typical of that in a passenger car, with a specially fabricated single-orifice nozzle. The orifice was 178 μm in diameter, and the injection pressure was selectable between 50 and 135 MPa. The fuel was injected into an x-ray-accessible spray chamber filled with an inert gas, sulfur hexafluoride (SF_6), at 1 atmospheric pressure and room temperature. The fuel used in this study was a blend of No. 2 diesel and a cerium-containing compound, with cerium concentration 4% by weight in the blend.

Two experimental arrangements were used. In the first, carried out at the APS 1-BM beamline, the injection apparatus was scanned through a small, focused x-ray beam. The transmitted beam was recorded using an avalanche photodiode (APD), which served as a fast point detector. At the D-1 beamline of CHESS, a wide bandpass (1%), extended size beam was used in conjunction with a fast pixel array detector (PAD). (The PAD detector was developed by Sol Gruner's group at CHESS.)

The combination of high-intensity x-rays from a synchrotron and the PAD allowed us to image the shock waves during the injection process. Figure 1.2 shows images of the fuel spray jet with the fuel injection pressure was set to 135 MPa. The leading edge of the fuel spray jet reaches 345 m/s and exceeds the sonic speed. The shock-wave front (the so-called Mach cone)

emanates from the leading edge of the fuel jet soon after emergence from the nozzle. Measurement of the Mach cone angles gives values that agree with the leading edge speed.

We also derived the mass density distribution of gas medium near and inside the Mach cone. In the plane perpendicular to the jet axis, the shocked region is a cone with an excess density in the SF_6 of $0.6 \mu\text{g}/\text{mm}^3$ measured 10.4 mm from the spray tip. Behind the high-density region, the interior of the cone has a small but observable reduction in the gas density from the ambient, which implies that decompression has occurred away from the Mach cone.

This study has paved the way to directly study the complete range of fluid dynamics inside and close to high-pressure liquid sprays. The time-resolved, radiographic method should also prove useful in characterizing highly transient phenomena of, and in, optically dense materials, such as dense plasma and complex fluid-gas interactions.

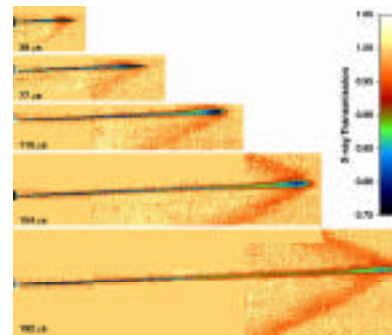


Fig. 1.2. Time-resolved radiographic images of fuel sprays and the shock waves generated by the sprays for time instances of 38, 77, 115, 154 and 192 μs after the start of the injection (selected from the total of 168 frames taken).

1.2.3 Crystal Diffraction Medical Imaging Lens

The first full-scale crystal-diffraction medical-imaging lens has been completed and tested. The lens consists of 13 concentric rings of copper single crystals aligned in such a manner that they all focus gamma rays or x-rays coming from a small source onto a small detector. The lens is capable of focusing x-rays and gamma rays with energies between 80 keV and 250 keV. The latest version of this imaging system is shown in Fig. 1.3. It is clear from this figure that the imaging system does not have to be close to the patient, eliminating any possible claustrophobia effect.



Fig. 1.3. The crystal diffraction medical-imaging lens system. The lens is located in the central cylinder section, the NaI detector is mounted at the upper end, and the breast phantom (with a small radioactive sample located inside) is shown below the end of the imaging system.

Tests of the imaging lens system were performed with energies of 121 keV (^{57}Co) and 141 keV (^{99}Tc), the latter being the most common source in medical imaging. Recent x-ray optics developments have reduced the spatial resolution to 3 mm FWHM (for a 1-mm-diameter source). This resolution is a factor of three better than most of the imaging systems in use today and is as good (and in most cases better) than the PET scanning instruments that are currently being developed.

The crystal-lens imaging system can be applied to small animals (e.g., rabbits, rats, or mice) that are used by the pharmaceutical industry for testing of newly developed drugs. It can also be used to image small parts of the human body such as blood vessels. Based on the data obtained with this lens, we are considering lenses with still better resolution, possibly as small as 1 mm FWHM. This resolution would allow the detection of very small tumors in places such as the female breast or in small test animals. There are many possibilities for nonmedical applications of such a lens system, including the examination of nuclear fuel elements and the location of radioactive material within a larger mass.

1.3 Time-Resolved X-ray Techniques Development

The time-resolved x-ray program can be divided into three parts: radiographic studies of fuel sprays, *in situ* measurements of nanoparticles in polymer-film systems, and x-ray streak camera development. Breakthroughs have been made in each of these areas during the time period covered by this report.